DOI: 10.17617/2.3194860
Proceedings of the 9th Solar Polarization Workshop SPW9
A workshop held in Göttingen, Germany, from August 26 to August 30, 2019
Achim Gandorfer, Andreas Lagg, Kerstin Raab (eds.)

Polarimetry with the GREGOR Fabry-Pérot Interferometer

H. Balthasar[1,*], D. Gisler[2,3], S. J. González Manrique[4], C. Kuckein[1], M. Verma[1], and C. Denker[1]

[1]Leibniz-Institut für Astrophysik Potsdam (AIP), Potsdam, Germany
[2]Istituto Ricerche Solari Locarno (IRSOL), Locarno-Monti, Switzerland
[3]Leibniz-Institut für Sonnenphysik (KIS), Freiburg, Germany
[4]Astronomical Institute of the Slovak Academy of Sciences, Tatranska Lomnica, Slovakia
[*]*Email:* hbalthasar@aip.de

Abstract. The polarimeter of the GREGOR Fabry-Pérot Interferometer (GFPI), which is attached to the 1.5-meter GREGOR solar telescope on Tenerife was upgraded in 2018. In addition to two ferroelectric liquid crystal retarders (FLCR), a fixed half-wave plate and a fixed quarter-wave plate were inserted to achieve high polarimetric efficiencies for the nominal spectral range of the GFPI (530–860 nm). In this contribution, we report how the modified polarimeter interacts with the telescope and the installed polarimetric calibration unit.

1 Introduction

The 1.5-meter GREGOR solar telescope (Schmidt et al. 2012) is equipped with the GREGOR Fabry-Pérot Interferometer (GFPI, Puschmann et al. 2012), among other post-focus instruments. The GFPI can be operated in spectroscopic or in spectropolarimetric mode. For polarimetry, a polarimeter has to be inserted in front of the camera of the narrow-band channel. Basically, the polarimeter consists of two ferroelectric liquid crystal retarders (FLCR) and a polarizing beam splitter (Bello González & Kneer 2008; Balthasar et al. 2011). In this beam splitter, two calcite blocks are combined at 180° with respect to each other, and to exchange ordinary and extraordinary beam from the first calcite, a half-wave plate is placed between them. This polarimeter can serve as a prototype for the European Solar Telescope (EST, Collados et al. 2010a,b; Jurčak et al. 2019). For polarimetric calibrations, GREGOR is equipped with two calibration units. One is placed in the secondary focus (Hofmann et al. 2012), the other one is located after the exit window of the coudé-train and before the derotator.

2 Modifications of the polarimeter

In 2016, we had to replace the FLCRs. The new ones were purchased from Meadowlark, and they were specified as zero-order half-wave and quarter-wave retarders at a wavelength of 630 nm. The wavelength for exact half-wave or quarter-wave retardance is between 680

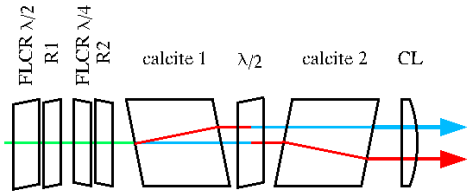

Figure 1. Scheme of the polarimeter. The additional retarders are marked by R1 and R2. The cylindrical lense is marked by CL.

and 700 nm, which is still within the tolerance specified by the manufacturer, and this is not a restriction for the performance of the polarimeter at 630 nm. However, without additional retarders the FLCRs provide useful polarimetric efficiencies only over a limited wavelength range (600–740 nm). Therefore we added two polymer zero-order retarders, which are placed behind each of the FLCRs. We combined a half-wave retarder at 488 nm (R1) with the half-wave FLCR and a quarter-wave retarder at 670 nm (R2) with the quarter-wave FLCR. To compensate for the astigmatism introduced by the calcites of the polarizing beam splitter, we added a cylindrical lense at the exit of the polarimeter. A scheme of the polarimeter is given in Figure 1.

The elements were tested at the Leibniz-Institute for Solar Physics (KIS) in Freiburg. We used a setup consisting of a fiber-coupled halogen light source, a collimator, a wiregrid polarizer, a motorized rotation stage, another polarizer, and a collector lens to feed a fiber towards a small spectrograph with a detector line. The element or combination of elements to be investigated was mounted on the rotation stage and rotated in steps of two or five degrees from zero to almost 360°. From these measurements we obtained the retardance and the orientation of the fast axis (with a 90° ambiguity). The ambiguity could be solved by inserting an additional quarter-wave plate. These results were used to calculate the polarimetric efficiencies of our polarimeter. Expected and measured curves are shown in Figure 2. The precise alignment between FLCR and additional retarder is difficult. Therefore, we show two different curves for two assumptions within the error margin of this alignment. The curves show that the polarimetric efficiencies are close to the expected ones and for wide ranges even above 0.5, for the whole wavelength range 530–860 nm, they are above 0.3. These results are obtained under laboratory conditions, valid for the polarimeter without the telescope.

3 Experience at the telescope

At the GREGOR telescope, we could take so far only a few measurements in two wavelengths in May 2018 and three different wavelengths in June 2019. For these measurements, we used the telescope calibration unit in the secondary focus (Hofmann et al. 2012). Efficiencies averaged over the two polarimetric channels and the available measurements are given in Table 1. Data for 630.2 nm were obtained in both years. The values for 630.2 nm are as expected, and those for 550.6 nm and 617.3 nm are in a reasonable range. Only for 543.4 nm, we encounter a rather low efficiency for Stokes-V. The value is below the expec-

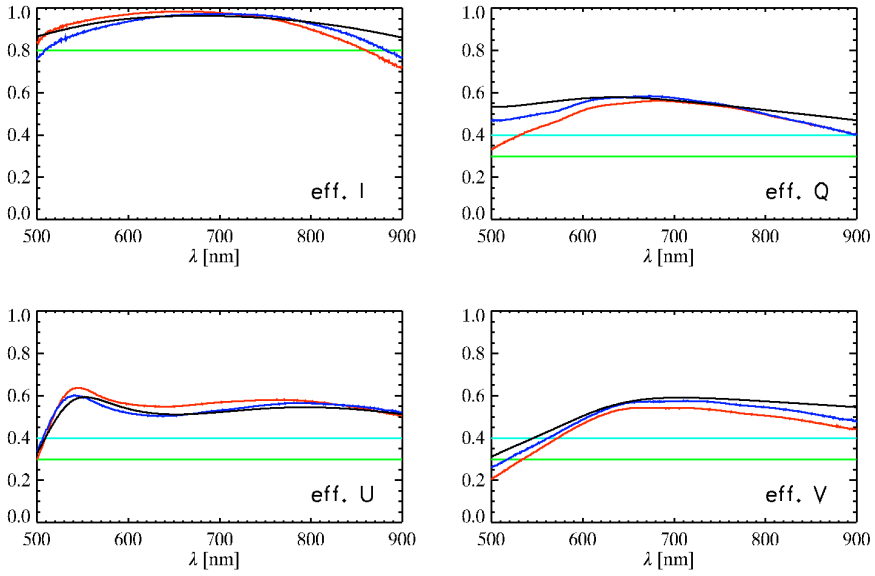

Figure 2. Expected *(black)* and measured polarimetric efficiencies for the GFPI-polarimeter *(red and blue)*. The horizontal lines indicate the thresholds of 0.3 and 0.4

Table 1. Polarimetric efficiencies at the telescope.

	543.4 nm	550.6 nm	617.3 nm	630.2 nm
n	1	7	1	16
I	0.70	0.87	0.85	0.82
Q	0.52	0.41	0.59	0.47
U	0.51	0.50	0.48	0.50
V	0.27	0.52	0.39	0.48
total	0.78	0.84	0.85	0.84

tation for the polarimeter itself, but the efficiencies vary with the telescope orientation. For the different wavelengths, we have different numbers of measurements (n in Tabel 1), and they were taken at different telescope orientations, which potentially affects the efficiencies. Therefore, we can deduce only a tendency with wavelength, but not a clear dependence.

The field dependency of the polarimetric efficiencies is displayed in Figure 3. We select as an example a measurement obtained in 2018 at a wavelength of 630 nm. The variation across the field-of-view is rather small and can be neglected for most cases. For shorter wavelengths, the variation is slightly larger, but it is still possible to perform an field-independent polarimetric calibration.

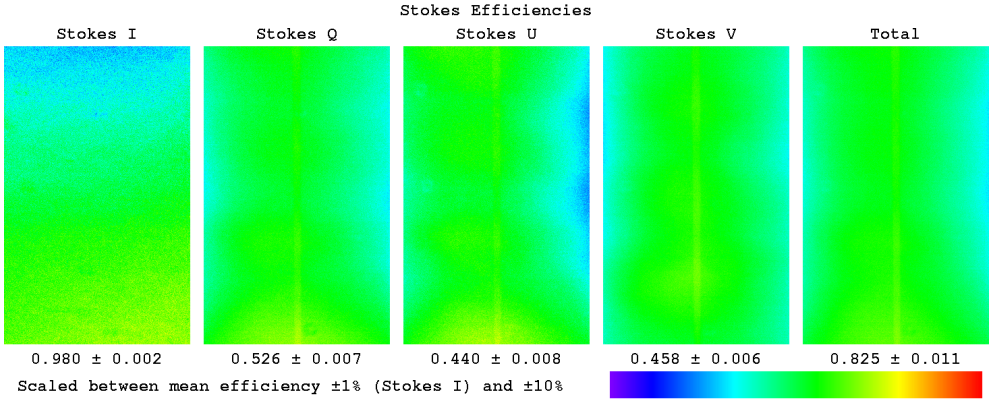

Figure 3. Field dependency of measured polarimetric efficiencies for 630 nm (single measurement).

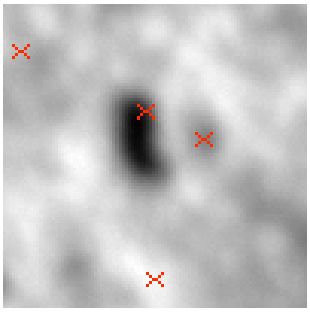

Figure 4. Image of the pore observed on June 05, 2019. One side of the image corresponds to 14.″5. Red crosses mark the positions where the profiles in Figure 5 were taken.

4 Test observation

The polarimetric calibration can be carried out in two different ways. If the required time for the science data is less than half an hour, two polarimetric calibration measurements with the telescope calibration unit immediately before and after the science data can be used. The applied calibration is an interpolation between these two calibration measurements. For longer durations of the science measurements or time gaps between calibration and science data recording, the internal rotations of a telescope in alt-azimuthal mount become too large, and a telescope model needs to be developed. To build a telescope model, several calibration measurements with different telescope orientations are required to fit the polarimetric properties of the mirror coatings. The properties of the derotator and the constant optical path behind the derotator can be determined using a second calibration unit inserted between the exit window of the telescope's coudé-train and the derotator. Such a telescope model still depends on wavelength! Further details of a telescope model will be discussed elsewhere.

Unfortunately, on only one occasion (June 5, 2019) we could test the first method on a solar target with a strong magnetic field. We observed a small pore around noon under rather

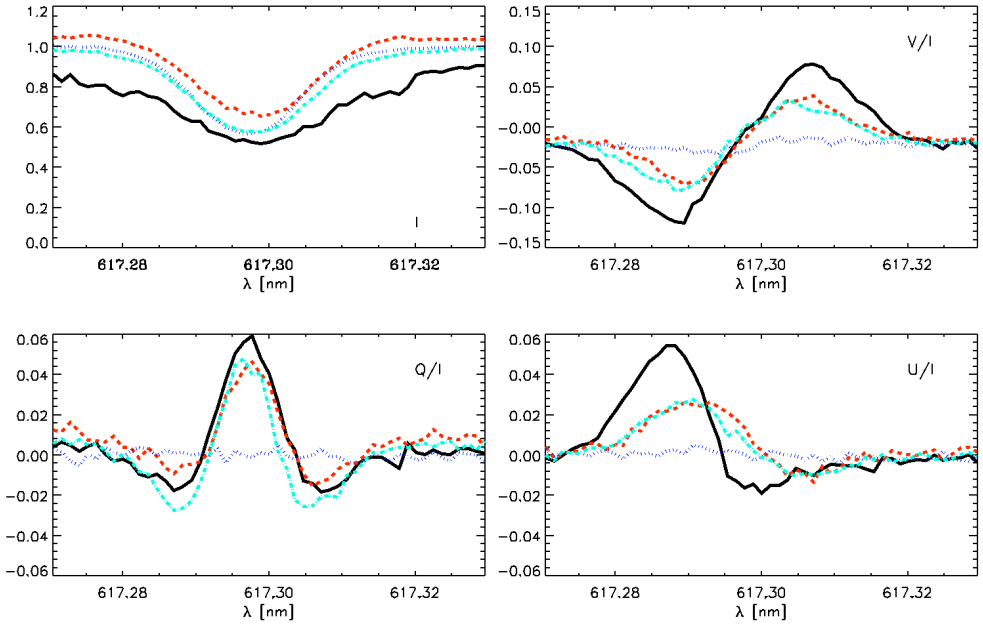

Figure 5. Stokes profiles for the main pore (solid black line), a micropore (turquoise dashes and dots), a nearby plage area (red dashes), and the quiet sun (blue dots). The positions are marked in Figure 4.

mediocre seeing conditions while we were still in the setup phase for the polarimeter. Thus we took a calibration only before the science recording. An image of the pore after 4×4 binning is shown in Figure 4. Since the seeing conditions were mediocre, we binned pixels to reduce the noise in the Stokes profiles. Four positions were selected for the Stokes-profiles displayed in Figure 5. We selected a position inside the main pore where we expect also linear polarization in Q and U. The other positions are in a dark feature (micropore) next to the main pore, in a bright plage area surrounding the main pore, and in the quiet Sun. Software tools to reduce the data are available in the sTools-package (Kuckein et al. 2017; Denker et al. 2018) and were applied to determine the Stokes profiles. Figure 5 shows the results for selected features in the field-of-view. For the main pore, we see regular Q and V profiles, but for U, we find irregular profiles. We also find regular V and Q profiles for plage and the micropore, but irregular profiles for U. In the quiet Sun, we see only noise for Q, U, and V. The U profiles can be explained with a remaining crosstalk from V to U, probably due to the missing calibration after the science data recording and the phase when the azimuth rotation is fastest for an alt-azimuthal mounted telescope. Adding a third of the V-profile yields a standard $-U$-profile for the main pore and noise-profiles for plage and micropore.

5 Conclusions

We demonstrate that the modifications of the GFPI-polarimeter work for the spectral range 550–860 nm, although one has to keep in mind that the transmission around 850 nm is low because of optical surface coatings in telescope and instruments, and the sensitivity of camera sensors based on silicon wafers is decreasing with increasing wavelength. Science data of limited duration up to half an hour can be reduced using two polarimetric calibration measurements with the telescope calibration unit just before and after recording the science data.

Acknowledgements. The 1.5-meter GREGOR solar telescope was built by a German consortium under the leadership of the Leibniz-Institut für Sonnenphysik (KIS) in Freiburg with the Leibniz-Institut für Astrophysik Potsdam (AIP), the Institut für Astrophysik Göttingen (IAG), the Max-Planck-Institut für Sonnensystemforschung in Göttingen (MPS), and the Instituto de Astrofísica de Canarias (IAC), and with contributions by the Astronomical Institute of the Academy of Sciences of the Czech Republic (ASCR). SJGM acknowledges the project VEGA 2/0048/20.

References

Balthasar, H., Bello González, N., Collados, M., et al. 2011, in Solar Polarization 6, ed. J. R. Kuhn, S. V. Berdyugina, D. M. Harrington, S. Keil, H. Lin, T. Rimmele, & J. Trujillo Bueno, ASP Conf. Ser., 437, 351

Bello González, N. & Kneer, F. 2008, A&A, 480, 265

Collados, M., Bettonvil, F., Cavaller, L., et al. 2010a, AN 331, 615

Collados, M., Bettonvil, F., Cavaller, L., et al. 2010b, Proc. SPIE 7733, 77330H

Denker, C., Kuckein, C., Verma, M., et al. 2018, ApJS 236:5

Hofmann, A., Arlt, K., Balthasar, H., et al. 2012, AN 333, 854

Jurčak, J., Collados, M., Leenaarts, J., et al. 2019, Advances in Space Research 63, 1389

Kuckein, C., Denker, C., Verma, M., et al. 2017, in Fine Structure and Dynamics of the Solar Atmosphere, eds. S. Vargas Domínguez, A. G. Kosovichev, L. Harra, & P. Antolin, Proceedings of the IAU Symposium 327, 20

Puschmann, K. G., Denker, C., Kneer, F., et al. 2012, AN 333, 880

Schmidt, W., von der Lühe, O., Volkmer, R., et al. 2012, AN 333, 796